



FINAL PUBLISHABLE REPORT

Grant Agreement number 18HLT02
 Project short name AeroTox
 Project full title Measurements for mitigating adverse health effects from atmospheric particulate pollutants

Project start date and duration:		1 June 2019, 42 months
Coordinator: Konstantina Vasilatou, METAS Tel: 0041 58 387 03 82 E-mail: konstantina.vasilatou@metas.ch		
Project website address: http://empir.npl.co.uk/aerotox/		
Internal Funded Partners:	External Funded Partners:	Unfunded Partners:
1. METAS, Switzerland 2. BAM, Germany 3. FMI, Finland 4. NPL, United Kingdom	5. FHNW, Switzerland 6. KCL, United Kingdom (withdrawn from 7 July 2020) 7. LUND, Sweden 8. UBERN, Switzerland 9. IC, United Kingdom (joined from 7 July 2020)	-
RMG: -		



TABLE OF CONTENTS

1	Overview	3
2	Need	3
3	Objectives	3
4	Results	4
4.1	Objective 1	4
4.2	Objectives 2 and 3	8
4.3	Objective 4.....	14
5	Impact	20
6	List of publications.....	21



1 Overview

Atmospheric particulate pollution has been linked to a broad spectrum of adverse health effects including respiratory problems, cardiovascular diseases, cancer and dementia. These effects depend not only on physical, but also on chemical properties of airborne particulate matter (PM) though to date it has proven difficult to disentangle the relative contribution of PM constituents to the reported population-level health effects. To address this issue this project used “tailored” reference aerosols, combined with high-resolution optical imaging of exposed cells and state-of-the-art cell analysis methods to study the cytotoxic effects of airborne PM *in vitro*. This was done in a systematic way to help inform which PM metrics are associated with the induction of toxic mechanisms so that they are linked to specific health effects. The project has developed new instrumentation, e.g. an automated oxidation flow reactor and a portable aerosol mixing chamber, and has shed light into the PM components that cause cytotoxic effects in *in vitro* studies.

2 Need

Airborne particles cause serious acute and chronic human health effects, associated with several hundred thousand premature deaths in the EU each year. For historical reasons, atmospheric particulate pollutants have been regulated for human health purposes by the mass concentration of discrete size fractions: PM₁₀ and PM_{2.5} (particles with diameter below 10 µm and 2.5 µm, respectively). However, PM mass concentration, fails to capture the chemical heterogeneity of airborne particulates and is uninformative concerning the toxicologically important contributions of ultrafine particles (<100 nm), which are of negligible mass. It has therefore been hypothesised that PM mass concentration, whilst useful, is not the most informative metric to characterise the potential of particles to cause the disparate detrimental health effects reported. The focus on mass also precludes the application of intelligent targeting of ‘health-relevant’ constituents. Therefore, there was a need to generate new data on the contribution of PM constituents to discrete toxicological relevant pathways. This can then be used to provide information on the causal link between the inhaled particles - and the down-stream health effects. Such information is vital if new metrics, such as particle size, number concentration and chemistry, are to be integrated into existing air quality guidelines.

The current literature evaluating the associations between air pollution and adverse health outcomes has been dominated by epidemiological studies, investigating the overall health effects of atmospheric air pollution, including particles, gases and mixtures. These studies, however, are limited in their capacity to distinguish independent effects of isolated aerosol components or properties on health. To disentangle the effects of the different aerosol properties on health, there is a need for well-defined reference aerosols generated in the laboratory. These aerosols should simulate the properties of real ambient aerosols whilst being stable and reproducible, with properties that can be “tailored” according to the experimental needs.

In vitro studies are essential for understanding the cause-effect relationship between airborne particles and cell/tissue damage. However, their value is fundamentally dependent on robust *in vitro* to *in vivo* correlation. To achieve this there is a need to go beyond the traditional cell-exposure techniques and simple biological models (e.g. 2D cultures). Novel methods for cell exposure that mimic the natural inhalation routes must be used and new biological models, such as lung organoids and lung scaffolds (3D multicellular structures), need to be developed to provide physiologically relevant models for measuring biological effects.

Cellular responses to pollutant stressors can be investigated with a combination of optical imaging techniques and biomedical assays. In both cases, quantification and integration of data from across multiple analytical platforms is challenging statistically and subject to measurement error and/or interpretive biases. For a meaningful integration of multiple endpoints to establish adverse outcome pathways (AOPs) in relation to specific PM properties and components, a metrology framework needs to be established to derive quantitative and reproducible response metrics.

3 Objectives

The overall goal of this project was to identify correlations between particle component/properties (metrics) with adverse outcome pathways that are associated with the induction of acute and chronic health effects within the European population. This was delivered through the development of a new method for studying *in vitro* cytotoxicity based on the use of “tailored” synthetic ambient aerosols combined with high-resolution optical imaging and state-of-the-art cell analysis methods. The specific objectives of the project were:



1. To develop a stable and reproducible laboratory-based source of well-controlled and chemically defined, synthetic reference aerosol mixtures that mimic real ambient aerosols at high concentrations (at around the limit values of the EU Air Quality Directive and up to a few mg/m^3). The aerosol properties should be tuneable and the source should be coupled to an oxidation flow reactor (OFR) to mimic atmospheric photochemical "ageing". To improve traceability for the physical and chemical characterisation of the synthetic aerosols using EU reference methods (target uncertainty in mass concentration 15 %, number concentration <15 %, analysis of major chemical components <15 %). Moreover, to quantify uncertainties for emerging techniques, such as Aerosol Mass Spectrometry (AMS) for chemical analysis and Brunauer–Emmett–Teller (BET) for surface area analysis and develop new approaches to ensure reproducibility and quality assurance.
2. To apply novel methods for cell exposure at the air-liquid interface (ALI) in order to mimic and quantify the effects of the in vivo aerosol inhalation routes. To study phenotypic effects using lung organoids. To compare these novel methods with the conventional cell-exposure techniques relying on submerged cell systems, where aerosol particles are collected in water with high-volume samplers.
3. To assess how the composition of the collected aerosols and their ageing impacts on their acellular and cellular oxidative characteristics, both in simple chemical models simulating human respiratory tract lining fluids (in health and disease) and in representative cell lines and lung tissue cultures maintained under near physiologic conditions. To evaluate adverse outcome pathways using proteomics and transcriptomics (high throughput sequencing), to examine known causal pathways, such as pro-/anti-inflammatory responses, cytotoxicity and genotoxicity, as well as novel 'component-specific' pathways. The project worked toward improved, validated protocols for harmonising/standardising cell analysis studies, as well as on the integration of multi-omic approaches for statistical analysis of complex data sets on a European level.
4. To push the frontiers of optical imaging and biological image analysis to quantify the effects of particle uptake on single cells and cell populations by using various types of optical microscopy including confocal, structured illumination, light sheet and fluorescence lifetime imaging.
5. To facilitate the take up of the technology and measurement infrastructure developed in the project by the measurement supply chain (accredited laboratories, instrumentation manufacturers), standards developing organisations (CEN, ISO) and end users (e.g. hospitals and health centres).

4 Results

4.1 Objective 1

4.1.1 Development of a portable flow tube homogenizer (aerosol mixing chamber)

A portable and light-weight aerosol homogenizer was designed and validated experimentally at METAS. The design relies on large-scale primary standards for particle number and mass concentration previously developed for metrology applications but the dimensions have been scaled down to produce a versatile and user-friendly apparatus for everyday applications in aerosol sciences.

A computer-aided design (CAD, Inventor Professional 2019, Autodesk, USA) of the portable aerosol flow tube homogenizer is shown in Figure 1. The homogenizer is a custom-made cylindrical stainless-steel tube, oriented vertically, with an inner diameter of 50 mm. As illustrated in Figure 1a, three versions of the homogenizer were built, with a distance d between the aerosol injection point and sampling probes of 75 cm, 57 cm and 35 cm, respectively. The tube is equipped with three identical inlets for the injection of primary aerosols, which are placed at the very top as shown in Figure 1b and c (marked in yellow). Since the distance between the inlets is much larger than their inner pipe diameter, no considerable agglomeration (internal mixing) of the injected aerosols is expected. Dilution air (filtered, humidity and temperature controlled) is delivered through seven additional inlets at a total flowrate of 20-40 L min^{-1} (marked in green in Figure 3b). The dilution air sweeps the particles down the tube, where they are further mixed by three turbulent air jets (total flow rate of 10-20 L min^{-1}). The three air-jet injection tubes are placed symmetrically around the homogenizer tube (Figure 1c). Note that the design of the aerosol and air-jet inlets has been optimised to facilitate construction and maintenance. The total flow rate of the homogenized aerosol is equal to 30-60 L min^{-1} plus the flows of the primary aerosols. The temperature and relative humidity of dilution and mixing air can be adjusted to simulate different



environmental conditions. The setup can accommodate up to four sampling ports at the bottom of the tube, directly above the aerosol exhaust.

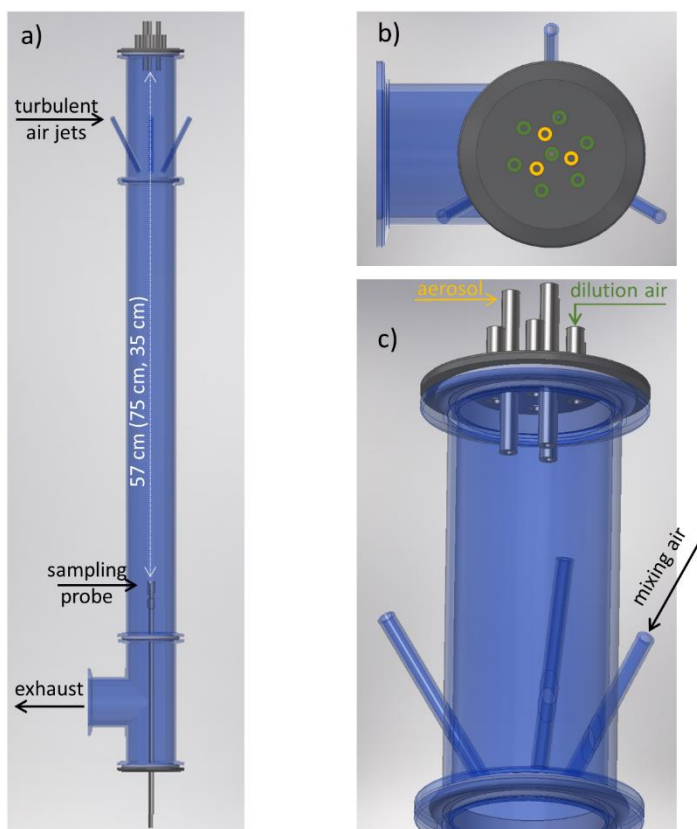


Figure 1. a) Computer-aided design of the aerosol flow tube homogenizer [3]. The distance between the aerosol injection point and the sampling probe d is 57 cm but other configurations with a distance of 75 cm and 35 cm were also tested (see text for more details). For simplicity, only one sampling probe is shown. Panel (b) shows a top-view image of the setup. The three aerosol inlets are marked in yellow and the seven inlets for dilution air are marked in green. Panel (c) shows an enlarged view of the upper part of the setup with the inlets for the primary aerosols, dilution air and mixing air. All components are made of stainless steel. The flow tube homogenizer and the inlets for mixing air are illustrated as transparent material for visualisation purposes only. This figure was first published in (Horender et al., 2022) and is licensed under a Creative Commons Attribution (CC BY) license.

The homogeniser was equipped with isokinetic sampling probes (Figure 2). Due to the small inner diameter (50 mm) of the portable homogenizer, only up to four isokinetic sampling probes for instruments with an aerosol flow of $\leq 3 \text{ L min}^{-1}$ can be accommodated. The inner diameter of each sampling cone was 10 mm, the outer diameter 12 mm and the distance between the funnels was 2 mm.

To characterize the aerosol spatial homogeneity in the flow tube as a function of particle size, polystyrene (PS) particles with a nominal geometric diameter of $2 \mu\text{m} - 5 \mu\text{m}$ were generated using a nebuliser (AKG2000, Palas Germany). Residue particles were filtered out with an aerodynamic aerosol classifier (AAC, Cambustion, UK).



Figure 2. Left panel: Picture of the portable flow tube homogenizer developed and constructed at METAS. Right panel: Isokinetic sampling probes for devices under test (left panel), and close view of the sampling funnel. The sampling probes were designed and constructed at METAS. This figure was first published in (Horender et al., 2022) and is licensed under a Creative Commons Attribution (CC BY) license.

The aerosol spatial homogeneity at the sampling zone was found to be within $\pm 1\%$ and $\pm 4\%$ for 2 and 5 μm PS (polystyrene) particles, respectively.

The homogenizer allows for mixing various aerosol components, such as soot, inorganic species and mineral dust particles to generate ambient-like aerosols in the laboratory or industrially manufactured particles such as polystyrene spheres as model aerosols. It can be applied in the aerosol health related-studies. It can serve as a useful tool for calibration of common aerosol instruments, such as portable PM mass monitors, optical and aerodynamic particle size spectrometers, and bioaerosol monitors.

More details on the design and validation of the portable flow tube homogenizer can be found in (Horender et al., 2022).

4.1.2 Development of an automated oxidation flow reactor

A novel automated oxidation flow reactor was designed by FHNW in order to generate a wide variety of secondary organic aerosol samples. The instrument is equipped with a humidifier, a dosing system for volatile organic precursors and an oxidation flow reactor (OFR) for generation of secondary organic matter (SOM). The instrument, known as organic coating unit (OCU, Figure 3), can produce homogeneously nucleated SOM particles or, used in combination with a standard combustion generator (e.g., a diffusion flame soot generator or any other seed particle), particles coated with a controlled amount of SOM. The physical and chemical properties of the generated particles can be controlled in a simple manner by selecting through a touch-screen target values for parameters, such as organic gaseous precursor concentration, humidity, and UV (ultraviolet) light intensity. Parameters and measured quantities are automatically stored in text files for easy export and analysis.

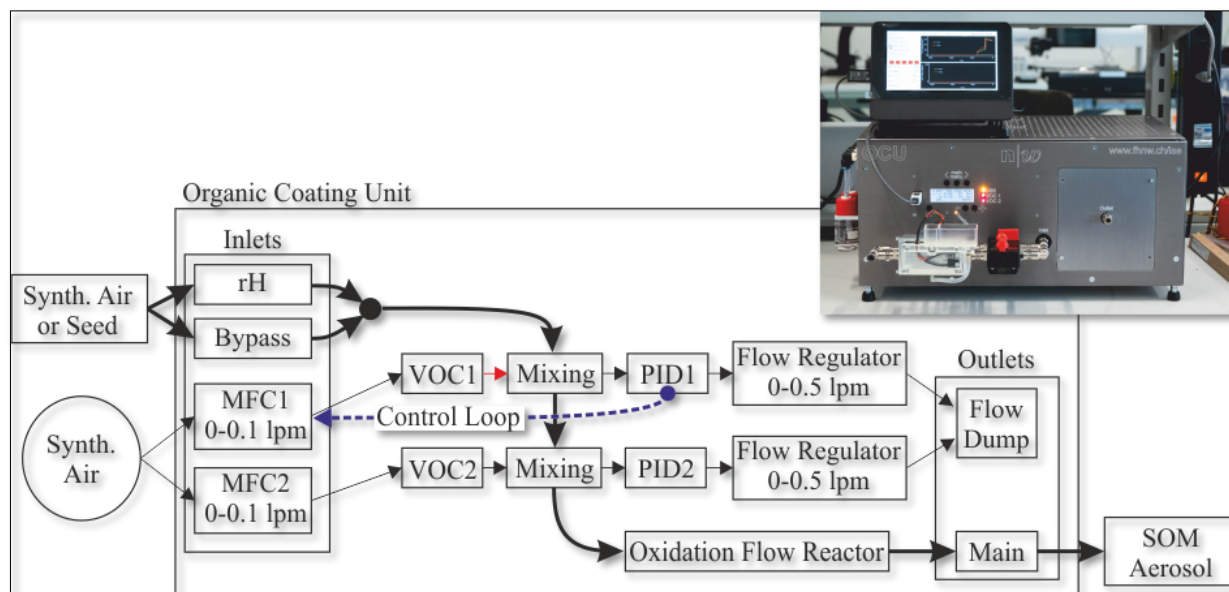


Figure 3. Schematic representation of the Organic Coating Unit (OCU) components. The main flow path is marked with thick arrows. Two different precursor VOC substances can be dosed at two sequential mixing points. The resulting mixture is then exposed to UV light in an oxidation flow reactor to generate SOM aerosol. Mass flow controllers (MFC1 and MFC2) provide dosing air to bottles containing VOCs (VOC1 and VOC2). Photoionization detectors (PID1 and PID2) monitor the gas-phase VOC concentration. The first dosing stage delivers the gas-phase VOC through a heated line (marked red) and is regulated to a specific target VOC concentration by a control loop. The flow through the PID sensors is controlled by flow regulation systems (indicated as Flow Regulator), consisting of a filter, a flow sensor, and a membrane pump. Flow ranges are given in liters per minute (lpm). The picture on the top right is the front view of the Organic Coating Unit, showing control panel, aerosol inlet, humidifier, and main outlet. The VOC bottles for precursor dosing are located on the left side of the device. The microcomputer running the graphical interface is placed on top of the device. This figure was first published in (Keller et al., 2022); licensed under a Creative Commons Attribution (CC BY) license.

The physicochemical properties of the generated aerosols were characterized by partner METAS and the University of Basel (project Collaborator) with an array of methods, including transmission electron microscopy (TEM), thermal-optical analysis and liquid chromatography coupled with mass spectrometry (LC-MS) and stable operation points were determined. More information can be found in (Keller et al., 2022).

This all-in-one instrument is robust, compact, portable, and user-friendly, making it ideal for laboratory or field-based aerosol studies. METAS, FMI and FHNW have already employed the OCU for producing synthetic aerosols to compare different Black Carbon monitoring instruments (Kalbermatter et al., 2022)

4.1.3 Physical and chemical characterisation of synthetic (ambient-like) aerosols

Synthetic (ambient-like) aerosols generated in the laboratory were used in controlled in vitro cytotoxicity studies (Leni et al., 2022). The expanded uncertainties in the determination of number and mass concentration of the synthetic aerosols were typically <8 %, well below the target uncertainty of 15 %. The expended uncertainties in the chemical characterisation of the aerosol were higher, at least 15 %. The table below, generated by NPL, sets out an estimated uncertainty budget for the analysis of a typical sample by Aerosol Mass Spectrometry (AMS). Note that uncertainty assigned to aerosol solubility is very challenging to estimate, so an cautious estimated expended uncertainty of 15 % relative has been applied.



Table 1:

		Expanded ($k = 2$) uncertainty / %			
Uncertainty contribution		WSOM/ SO ₄ ²⁺	WSOM/ WSOC	O/C	H/C
C (NH ₄) ₂ SO ₄	Mass concentration of (NH ₄) ₂ SO ₄ solution (dilution)	1	<i>n/a</i>	<i>n/a</i>	<i>n/a</i>
AS	Aerosol solubility	15	15	15	15
R	AMS Repeatability factor	8	4	2	4
IE	Ionisation efficiencies	20	<i>n/a</i>	<i>n/a</i>	<i>n/a</i>
W	Weighted mass spectral fragment summation	<i>n/a</i>	8	12	4
Total estimated expanded uncertainty		26	17	19	16

The PAH (polycyclic aromatic hydrocarbon) content of the fresh soot particles was determined by partner FMI using Gas Chromatography coupled to Mass Spectrometry (GC-MS). The relatively high uncertainties (15-45 %; 95 % confidence level) in the determination of PAH were due to the very low PAH concentration on the surface of the synthetic soot particles generated by the miniCAST burner. Note that we had deliberately optimised the miniCAST operating points in such a way as to minimise production of PAH when generating soot particles. This allowed us to generate relatively "clean" soot particles with a high fraction of elemental carbon, which acted as nucleation cores for secondary organic matter.

More information on the physicochemical characterisation of the synthetic aerosols used for in vitro cytotoxicity studies can be found in (Leni et al., 2022). Having these results, the project successfully achieved the objective.

4.1.4 Summary

WP1 succeeded in delivering a fully automated oxidation flow reactor for the controlled generation of SOM and a portable aerosol homogeniser. Moreover, the uncertainties of various analytical methods were quantified and, where possible, reduced. Considering that both the new oxidation flow reactor and the portable homogeniser have already found multiple applications outside of the AeroTox project, WP1 has met or even exceeded the expectations related to Objective 1.

4.2 Objectives 2 and 3

4.2.1 First joint AeroTox project in vitro cell exposure campaign

Secondary organic matter (SOM) formed from gaseous precursors constitutes a major mass fraction of fine particulate matter. However, there is only limited evidence on its toxicological impact. In the first measurement campaign for the present project, air-liquid interface cultures of human bronchial epithelia were exposed to different series of fresh and aged soot particles generated by a miniCAST burner combined with a micro smog chamber (MSC). The work was conducted by METAS and UBERN. Soot cores with geometric mean mobility diameter of 30 nm and 90 nm were coated with increasing amounts of SOM, generated from the photo-oxidation of mesitylene and ozonolysis of α -pinene. ALI cultures of normal HBE were exposed to the different reference aerosols using the Nano Aerosol Chamber for In-Vitro Toxicity (NACIVT), allowing realistic delivery of (nano)particles out of a conditioned air-flow to the apical surface of ALI (Air-Liquid Interface) cell cultures. At 24 h after exposure, the release of lactate dehydrogenase (LDH), indicating cell membrane damage, was



measured and proteome analysis, i.e. the release of 102 cytokines and chemokines to assess the inflammatory response, was performed.

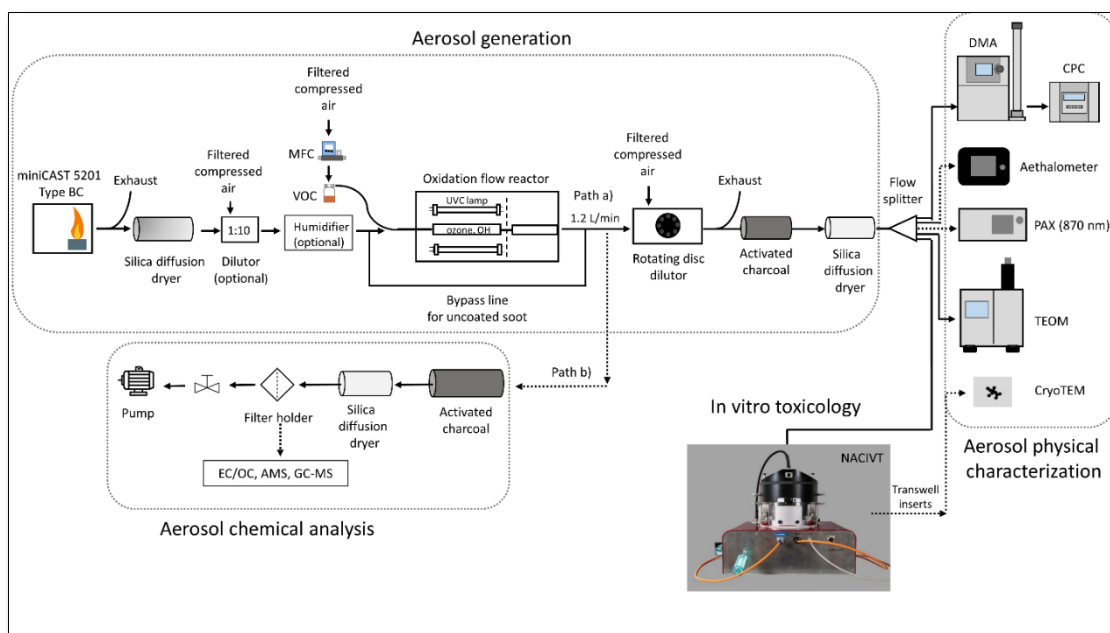


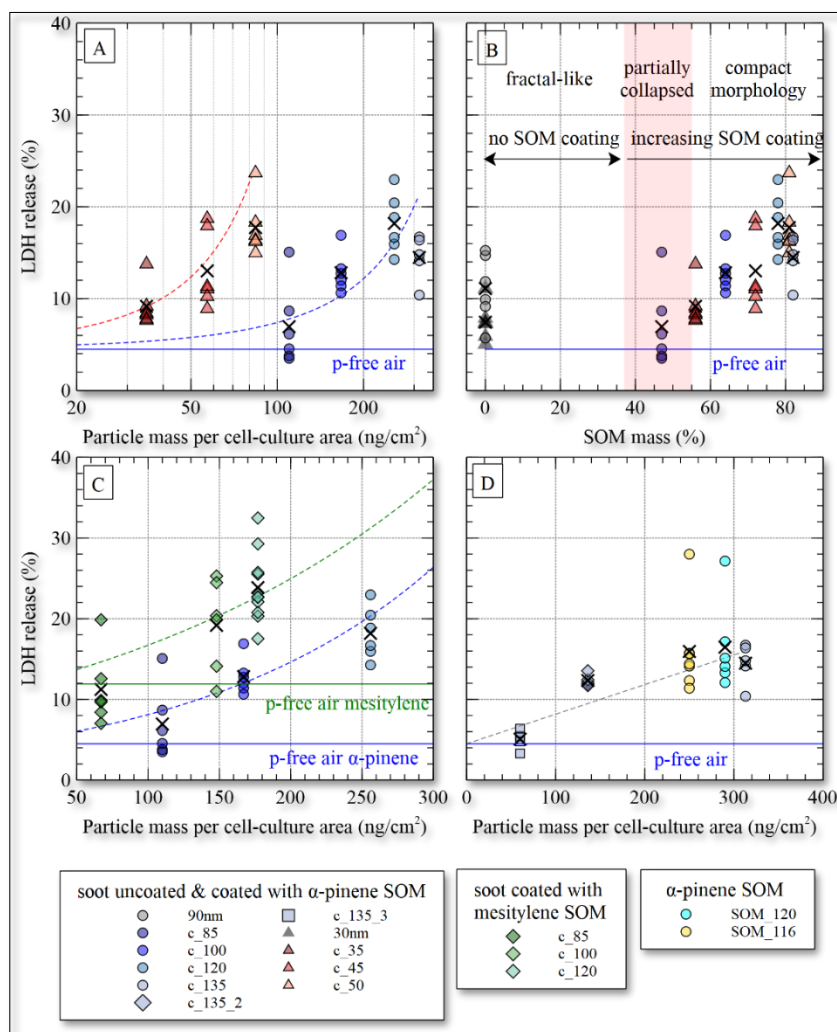
Figure 4. Schematic illustration of the experimental setup for aerosol characterization and cell exposure in the NACIVT chamber. For experiments with uncoated soot, the oxidation flow reactor was by-passed. During cell exposure, we solely used the instruments connected with solid lines. For aerosol characterization, the additional instruments connected with dotted lines (PAX and AE33) were used. This figure was first published in (Leni et al., 2022) and is licensed under a Creative Commons Attribution (CC BY) license.

The experimental setup (Figure 4) allowed to accurately control the amount of SOM condensed on the core particles. This enabled the reproducible generation of different model aerosols with well-defined SOM mass/total particle mass ratios. The data indicated that the increase in total particle mass concentration alone cannot explain the observed trends in LDH release (Figure 5A). The chemical composition of the coating and its bioavailability seems to be important for cytotoxicity. The release of LDH was found to increase with increasing SOM mass/total particle mass ratio, but only when SOM had condensed on the outer surface of the soot cores (Figure 5B). Moreover, exposure of HBE to soot particles coated with SOM from the oxidation of mesitylene and the ozonolysis of α -pinene resulted in similar increase in LDH release compared to the control with particle-free air, under the experimental conditions used in this study (Figure 5C). The presence of the soot core seemed to have little or no effect on cytotoxicity, when it was fully embedded in SOM.

In addition, the inflammatory response of HBE by semi-quantitatively measuring the release of 102 cytokines and chemokines into the basal media was assessed at 24 h post-exposure. The activation of pro-inflammatory mediators may lead to a systemic inflammatory response. The results showed that both HBE exposed to soot coated with SOM from the oxidation of α -pinene and of mesitylene exhibited pronounced secretion of cytokines and chemokines compared to unexposed as well as p-free air exposed HBE. Consequently, there is a need to discriminate cytokines and chemokines regarding their involvement in biological processes concurrently with the magnitude of the effect. This analysis revealed a considerable number of deregulated cytokines (mainly upregulation) in comparison to unexposed HBE. The proteome screening revealed common signatures of deregulated proteins for both types of coated soot particles (biogenic and anthropogenic VOC) compared to the controls (unexposed and p-free air exposed HBE). In line with the data on the chemical composition, the biological results revealed a more pronounced cellular response upon exposure to 30-nm soot particles from biogenic or anthropogenic derived SOM. These data clearly demonstrate an increase in cytotoxicity, as well



as of cell remodeling and inflammatory processes upon exposure to the aerosols with 30-nm particles but not for the 90-nm series.





These findings highlight the role of SOM for in vitro toxicological outcomes and suggest that, in addition to total particle mass concentration, the percentage of the SOM fraction in $PM_{2.5}$ may be a useful metric to characterize the potential of particles to cause adverse health effects.

A detailed description of the experimental setup, the aerosol properties and the results of the cell analysis can be found in (Leni et al., 2022).

4.2.2 Second AeroTox project joint cell exposure campaign: Novel methods of cell-exposure at the ALI for 2D cell cultures and ex vivo lung explants

A joint campaign for Aerosol toxicity studies took place at NPL (National physical Laboratory, UK) during spring 2022, supported by partners LUND, IC, FHNW, METAS and BAM. Respiratory cell models were exposed to synthetic "fresh" and "aged" aerosols at the air-liquid interface inside an environmentally controlled deposition chamber (NACIVT). Online aerosol monitoring, combined with calibration of particle deposition rates within the chamber, allowed precise determination of the administered particle dose. Additional properties (particle size, elemental to total carbon ratio, single-scattering albedo and absorption Ångström exponent) of uncoated and coated soot particles were also characterised. See figure 2. This system was used to measure the response of A549 (human lung carcinoma epithelial), BEAS-2B (human bronchial epithelial), HFL1 (human lung fibroblast) and TT1 (human lung alveolar) cell lines to exposure with two different concentrations of uncoated soot and soot particles coated with biogenic secondary organic compounds. The cell lines A549, BEAS2B and HFL1 had previously been studied in the submerged intercomparison study and will be further evaluated here. TT1 had not previously been studied in the project but was included by Imperial College London (IC) as these cells best mimic the alveolar type 1 cells, a cell type that are difficult to culture. The cell culturing was organised at NPL with inputs from various partners. TT1 was provided by IC and lung scaffolds were provided by the University of Lund (LUND). TT1 was seeded in the scaffolds as a comparison to the mono-cultured TT1 cells.

Post exposure cytotoxic responses were measured using a variety of approaches including cell proliferation assays (WST-1) and proteomics and transcriptomics analysis. A subset of samples was fixed and stained for high resolution fluorescence microscopy analysis. Results were analysed to assess the relative toxicity of different particulates and the differential response of different cell types, indicating that TT1 cells are the most sensitive ones with reduced viability already after 24 hours to higher concentrations of biogenic coating, whereas reduced cell viability was observed for TT1 cultured in scaffolds and in BEAS2B and HFL-1 after 72 hours' exposure, showing the importance of also include longer exposure times. We also compared our data with similar studies performed using submerged cell culture models. In addition to providing data on the toxicity of coated and uncoated soot particles, our results can also be interpreted to develop improved respiratory toxicology screening protocols. This work was presented at the IAC conference in Athens (September 2022) and a manuscript is in preparation. Studies were also performed by IC on human primary dendritic cells from healthy donors that are exposed to the collected cell suspensions from SOA coated soot and uncoated soot exposed epithelial cells in the NACIVT study at NPL which are analysed by transcriptomics.

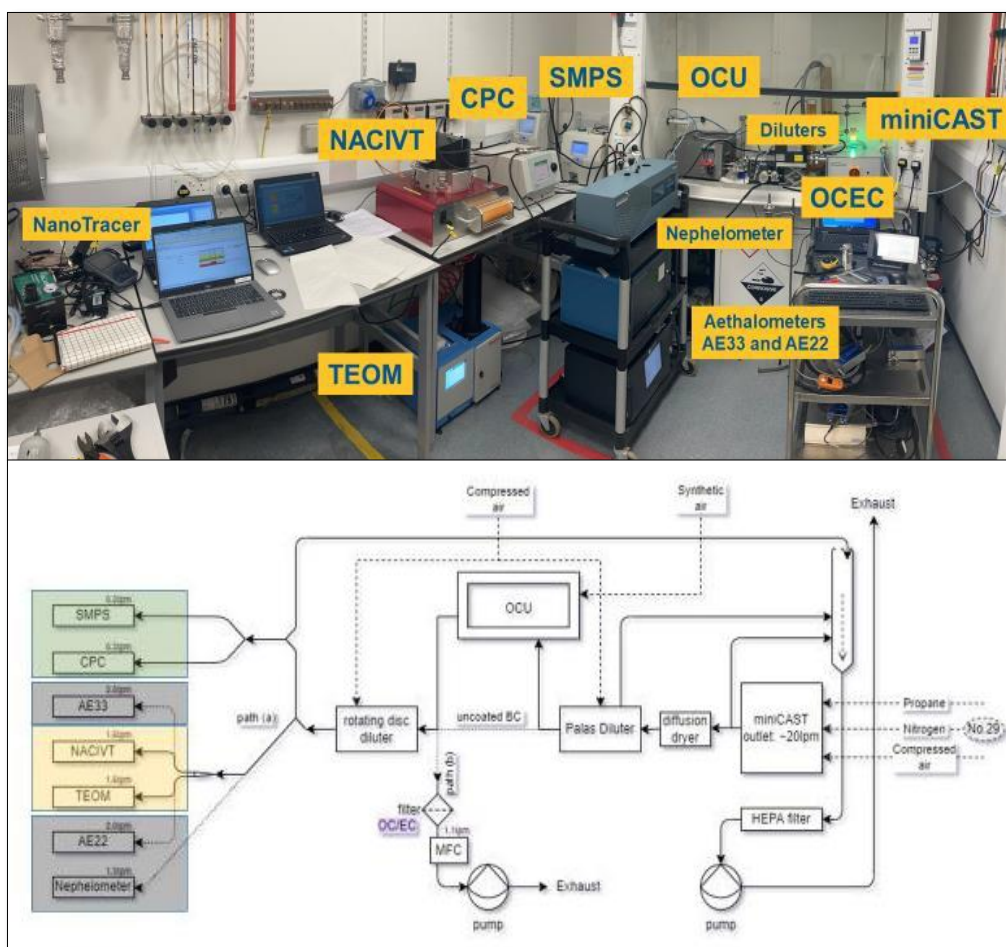


Figure 6. Set up of the exposure campaign with uncoated and coated soot particles at NPL in spring 2022.

4.2.3 Comparison of different cell-exposure methods

A study was performed by LUND to compare the toxicological responses to ZnO nanoparticle (NP) exposure in the NACIVT chamber (i.e. exposure at ALI) with two different submerged exposure systems at three different doses. The primary site of respiratory NP deposition during inhalation exposure is in the distal airways, which were represented by the use of human alveolar epithelial cells (A549) in our study. The results showed that the medium dose ($1.0 \mu\text{g}/\text{cm}^2$) used in the NACIVT system generated a significant increase in metabolic activity and release of IL-8 and MCP-1 as compared to the unexposed controls, while no significant increases could be seen in the two submerged systems at this dose. This indicates that the NACIVT exposure system may be more sensitive than the two submerged exposure systems, likely since it utilizes a more physiologically realistic exposure model. For more information the readers are referred to (Loven et al, 2021).

A small pilot study was also performed with PCLS in the NACIVT chamber indicating that the lung slices did maintain viability at air-liquid interface during one hour of aerosol exposure as there were no differences in viability (metabolic activity) between unexposed and exposed lung slices.

4.2.4 Intercomparison studies of submerged 2D and 3D in vitro systems

Toxicity studies with silver nanoparticles (AgNPs with the size 10 nm and 75 nm and two different concentrations 2 and $10 \mu\text{g}/\text{mL}$) were performed by LUND to compare responses in vitro and ex vivo. Results from *in vitro* cell cultures with human lung fibroblasts (HFL-1) and ex vivo lung tissue cultures with precision



cut lung slices (PCLS) indicated that AgNPs at higher concentrations induced cytotoxic effects, measured as increased LDH release and reduced metabolic activity in HFL-1 and PCLS after 48 h. These data indicate mitochondrial dysfunction which was visualized with TEM images. AgNPs significantly increased procollagen I synthesis and release of IL-8, prostaglandin E₂, RANTES and eotaxin, whereas reduced IL-6 release was observed in HFL-1 after 72 h. Hence, careful characterizations are of importance and we decided that future exposure studies with this project samples should include time points beyond 24 hours. For more information the readers are referred to (Löfdahl et al, 2020).

Optimising the *in vitro* culture system with lung tissue scaffolds was performed by LUND (Lung Biology group) to successfully obtain novel *in vitro* models for exposure studies with this project samples (lung scaffolds with TT1 cells exposed to soot particles). Human lung fibroblasts and mast cells were cultured on cell culture plastic plates or decellularized human lung tissue (scaffolds) to create a more physiological milieu by providing an alveolar extracellular matrix (ECM). Culture in scaffolds altered the release of mediators compared to classical cell culture on plastic plates. These data indicate a modulatory role by the alveolar ECM microenvironment in the interplay between resident and inflammatory cells, highlighting the importance of advancing work with more complex culture systems such as the 3D lung scaffold to increase the *in vivo* relevance of cell physiology studies *in vitro*. More details can be found in (Bagher et al, 2021).

LUND has also worked on the development of a bioreactor. A new prototype has been constructed to mimic breathing movements *in vivo* in the cell culturing. Our data indicate that culturing cells on human lung scaffolds with dynamic stretch mimics tidal breathing and induce increased surfactant production. Particle exposure with soot was done in a limited amount of samples in the bioreactor. Breathing exposes lung cells to continual mechanical stimuli, which is part of the microenvironmental signals directing cellular functions together with the ECM. Therefore, developing systems that incorporate both stimuli are urgent to fully understand cell behaviour. This study aims to introduce a novel *in vitro* culture methodology combining a cyclic stretch that simulates *in vivo* breathing with 3D cell culture platforms in the form of decellularized lung slices (DLS), also known as lung scaffolds, and precision cut lung slices (PCLS). To this end, we have constructed a device that mimics the amplitudes and frequencies of distensions seen in the breathing human lung. For its validation, we cultured H441 lung epithelial cells in human DLS exposed to 16 stretch cycles per minute with a 10% stretch amplitude. Cell viability (resazurin reduction), proliferation (Ki-67) and YAP1 activation were evaluated at 24 and 96 h by immunohistochemistry, while the expression of SFTP, COL3A1, COL4A3 and LAMA5 was evaluated by qPCR. Cyclic stretch induced an increase in SFTP expression after 24 h without a concomitant increase in the stretch responsive gene YAP1. Moreover, the ECM milieu lowered the expression of the basement membrane protein genes COL4A3 and LAMA5 compared to tissue culture plastic control cultures, but no effect was observed by the mechanical stimuli. The device also confirmed good compatibility with PCLS culture, showing preserved morphology and metabolism in rat PCLS after 72 h of mechanical stretch. Thus, we present a novel device and methodology for the easy assembling and study of lung tissue slice cultures subjected to physiometric mechanical stimuli, which shows promise for future studies of cell and tissue function in a lung ECM milieu with physiological or pathological mechanical stimuli. More details are available in Rosmark et al, 2022.

4.2.5 Inter-comparison study to establish the equivalence of the validation measurements for cytotoxicity and inflammatory markers and the biological model culturing between the partners.

An aerosol toxicity study using submerged systems with cultured A549 (human lung epithelial) cells, BEAS2B (human bronchial epithelial cells), H441 (human lung alveolar cells) and HFL1 (human lung fibroblasts) and the *ex vivo* model PCLS (precision cut lung slices) was performed. As an intercomparison study between the different partners, cells were exposed to various aerosol components (uncoated fresh soot particles, copper oxide, ammonium sulphate and ammonium nitrate) with three different concentrations of each component for 5-72 hours. Toxicity studies using submerged systems with cultured A549 (human lung epithelial) cells, H441 (human lung epithelial cells), THP-1 (macrophages) and HFL1 (human lung fibroblasts) and the *ex vivo* model PCLS was performed by different project partners. Exposure studies were also performed on H441 cells cultured in lung scaffolds (decellularised human lung tissue) and compared with H441 cultured on traditional plastic cell culture plates. Changes in cytotoxicity (LDH), metabolic activity (WST-1), generation of oxidative stress and immune responses



were analysed. Obtained results indicate that there are significant differences in toxicity of PM components and cellular responses that can be linked to adverse health effects. Cytotoxic responses were more pronounced in epithelial cells than fibroblasts and macrophages. Intercomparisons were also made between two metabolic assays: WST-1 and Presto Blue, which indicated that Presto Blue was less sensitive than WST-1 to detect metabolic alterations, highlighting that WST-1 should be recommended for identifications of mitochondrial dysfunctions, whereas Presto Blue is less harmful and may be useful for general viability check. Overall, fresh uncoated soot particles and copper oxide concentration-dependently induced toxicity, reduced metabolic activity related to mitochondrial dysfunction, increased ROS and altered immune response. Increased ROS generation and mitochondrial dysfunctions are well known features in COPD pathology. A manuscript is currently in preparation.

4.2.6 *In Vitro* Respiratory Models for respiratory toxicology

In summary, different *in vitro* respiratory models are used depending on the research question(s) and mechanisms that are investigated for respiratory toxicology. Table 2 gives an overview of advantages and disadvantages of different *in vitro* and *ex vivo* models for respiratory toxicology.

Table 2: Summary of the principal advantages and disadvantages of different *in vitro* and *ex vivo* models for respiratory toxicology.

Model type	Advantages	Disadvantages
Submerged 2D cell cultures	<ul style="list-style-type: none"> • Easy to prepare mono-cultures or co-cultures. • Compatible with high throughput screening systems. 	<ul style="list-style-type: none"> • Fails to recapitulate the 3D <i>in vivo</i> environment. • Difficult to mimic real world exposures.
Air-liquid interface cultures	<ul style="list-style-type: none"> • Mimics the <i>in vivo</i> epithelium. • Realistic exposure of cells to a range of aerosols. • Longer culture periods to study remodelling processes. • Compatible with advanced co-cultures and a range of cell types. 	<ul style="list-style-type: none"> • Feasible for studying exposure effects (only) on epithelial cells. • Lacks a 3D micro-environment
Spheroids and organoids	<ul style="list-style-type: none"> • Recapitulates cell-cell and cell-ECM interactions. • 3D environment to study EMT (epithelial – mesenchymal transition) processes. 	<ul style="list-style-type: none"> • Simplified 3D system lacking vascularization and physiological function.
3D cell scaffolds	<ul style="list-style-type: none"> • In vivo-like 3D architecture with a mono-, co- or multi-culture of cells 	<ul style="list-style-type: none"> • Lacks circulating immune cells. • Limitations in mimicking physiological function.
PCLS	<ul style="list-style-type: none"> • Snapshot of the lung with intact cellular architecture and biological processes. • 3D model that most closely resembles the <i>in vivo</i> system. 	<ul style="list-style-type: none"> • Lack circulating immune cells. • Shorter lifetime than other models. • Complex and heterogeneous. • Requires fresh lung tissue.

With the two successful joint measurement campaigns and more than 6 peer-reviewed papers already published or in preparation, WPs 2 and 3 have largely achieved the objectives 2 and 3.

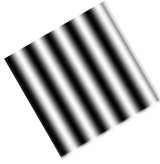
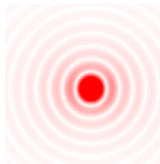

4.3 Objective 4

4.3.1 Microscope systems

The SIM, CLSM and LSM techniques described in this section differ significantly in key performance characteristics such as their spatio-temporal resolution, imaging field of view, depth penetration and the irradiance to which the sample is exposed during image capture. Some of the key characteristics are summarised in Table 3.



Table 3. Summary of the fluorescence microscope systems used to image the uptake and effect of particle exposure on respiratory models

<p>Super-resolution structured illumination microscopy (SIM)</p> <ul style="list-style-type: none"> Summary: Widefield inverted microscope. Spatial resolution is doubled using patterned illumination. Short to medium duration timelapse imaging of live cells Key specifications: ~100 nm (lateral) x ~500 nm (axial) resolution at up to 20 frames per second over a 35 μm x 35 μm field of view (1024 x 1024 pixels) Excitation lasers: 405 nm, 488 nm, 561 nm, 638 nm Sample mounting: samples should be mounted on #1.5 (preferably #1.5H) glass coverslips or in chambered coverslips such as the μ-Slide 8 well glass bottom from Ibidi (https://ibidi.com/glass-bottom/183--slide-8-well-glass-bottom.html). Fixed samples should ideally be mounted in an antifade reagent such as ProLong Gold (https://www.thermofisher.com/order/catalog/product/P36930) 	
<p>Confocal laser scanning microscopy (CLSM)</p> <ul style="list-style-type: none"> Summary: Point scanning inverted microscope well suited to imaging thick, densely labelled samples. Long duration timelapse imaging of live cells. Key specifications: highest achievable spatial resolution is ~200 nm (lateral) x ~500 nm (axial) at up to 28 frames per second (512 x 512 pixels) Excitation lasers: 405 nm, 448 nm, white light laser (485 nm to 685 nm) Sample mounting: samples should be mounted on #1.5 (preferably #1.5H) glass coverslips or in chambered coverslips such as the μ-Slide 8 well glass bottom from Ibidi (https://ibidi.com/glass-bottom/183--slide-8-well-glass-bottom.html). Fixed samples should ideally be mounted in an antifade mountant such as ProLong Gold (https://www.thermofisher.com/order/catalog/product/P36930) 	
<p>Light sheet microscopy (LSFM)</p> <ul style="list-style-type: none"> Summary: Fast 3D imaging with low sample light exposure over large sample volumes with upright geometry Key specifications: ~ 1 μm isotropic spatial resolution at 100 frames per second with ~ 1mm field of view Excitation lasers: 405 nm, 488 nm, 561 nm, 640 nm Sample mounting: Samples must be immersed in water / media of similar refractive index and fit into the 'imaging pocket' between excitation and detection objective lenses (see Figure 1 below). Typically this is achieved by mounting the sample within 1% agarose on a PDMS plinth, itself inside a shallow plastic dish. Samples mounted / cultured in other hydrogel systems (e.g. Matrigel) can also be imaged directly provided the gel can be mounted on top of a PDMS plinth. 	

4.3.2 Sample mounting

For exposure in submerged culture, cells were grown in #1.5H 8-well chambered coverslips (Ibidi) with particulate suspensions added directly to the cell culture medium. Following fixation and fluorescent staining (DAPI - DNA and MitoTracker Deep Red – Mitochondria) samples were washed and dried before an antifade mounting medium (ProLong Gold, ThermoFisher Scientific) was added on top. Samples were then imaged directly on inverted SIM and CLSM systems.

Air-liquid interface exposures were performed using the Nano Aerosol Chamber for In-Vitro Toxicology (NACIVT). Cells were cultured on Transwell inserts (Corning). After aerosol exposure and subsequent incubation, cells were fixed and stained for DNA (DAPI), Mitochondria (MitoTracker Deep Red), E-cadherin (primary-secondary antibody staining with AlexaFluor 488) and endosomes (Transferrin-AlexaFluor 488). The polymer membranes from the Transwell inserts were then removed using a scalpel and mounted between a microscope coverslip (#1.5H) and glass slide with antifade mounting medium (ProLong Gold).

HFL1 cells cultured in ~ 350 μ m thick sections of decellularised lung tissue were supplied in ethanol by Lund University. For LSFM imaging a 1 mm disc was cut from the tissue using a biopsy punch. After washing in MilliQ the cut sections were mounted in 1 % agarose on top of a cylindrical PDMS column bonded to a black



polystyrene weigh boat, itself glued onto a glass microscope slide. Once fitted onto the microscope sample stage, the weigh boat was filled with phosphate buffered saline solution to a level which covered the agarose containing the lung scaffold and the end faces of the two (excitation and detection) water dipping objective lenses.

4.3.3 Submerged 2D cell cultures

Figure 7 shows images of adenocarcinomic human alveolar basal epithelial (A549) cells exposed to copper oxide particles in suspension. In Figure 7 (a) and (b) cells were exposed to 1 $\mu\text{g/ml}$ of particles and cultured for 1, 2 and 3 days prior to fixation. Particles, and particle clusters, are visible both inside / on top of the cells and on the substrate as dark blobs / patches. In the SIM images (Figure 7(b)) individual mitochondria are clearly visible and present the characteristic spheroidal morphology expected for this cell line. Consistent with a WST-1 assay which indicated reduced cell viability upon exposure to copper oxide particles (data not shown), Figure 7 (d) shows that mitochondrial morphology is disrupted when the cells are exposed to a high (25 $\mu\text{g/ml}$) particle concentration.

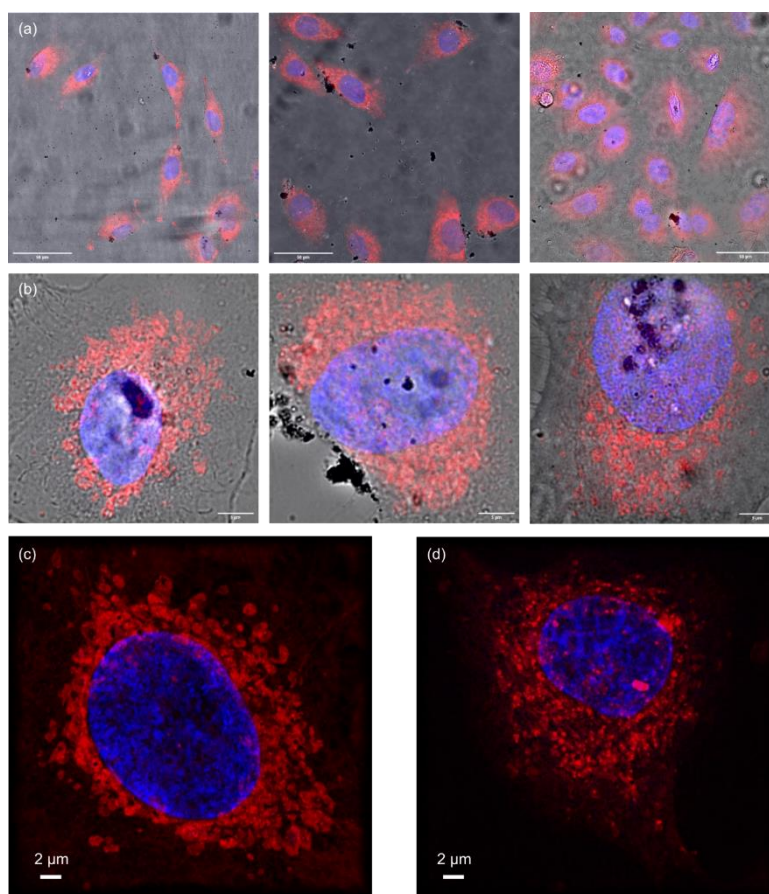


Figure 7. Optical microscopy images of A549 cells exposed to copper oxide particles. Brightfield images shown in grayscale, fluorescence microscopy image channels in red (MitoTracker Deep Red) and blue (DAPI). (a) Images of cells exposed to a low concentration (1 $\mu\text{g/ml}$) of CuO particles captured using laser scanning confocal microscopy. (b) Images of cells exposed to a low concentration (1 $\mu\text{g/ml}$) of CuO particles captured using SIM. (c) SIM image of a control cell not exposed to particles. (d) SIM image of a cell exposed to a high concentration (25 $\mu\text{g/ml}$) of CuO particles.



4.3.4 Air-liquid interface cultures

To image cells exposed at the air-liquid interface the polymer membranes were removed from Transwell inserts and mounted between a coverslip and microscope slide. We found this to be essential, as attempts to image cells directly through the membrane within the intact insert resulted in poor image quality due to light scattering by the membrane and a high autofluorescent background, as well as potential imaging aberrations caused by differences between the refractive index of the membrane and the imaging buffer.

Figure 8(a) shows example SIM images of E-Cadherin expression in A549 cells. E-cadherin is a membrane protein which plays an important role in cell adhesion, thus enables visualisation of the junctions between different cells. Staining and / or protein expression levels were inconsistent across the insert substrate making it challenging to develop a clear picture of how it is impacted by exposure of cells to aerosol particles. Figure 8(b) shows mitochondria in HFL1 cells. The elongated, filamentous, morphology of the mitochondria in this cell line shows a striking contrast with the more rounded morphology of mitochondria in A549 cells (Figure 7). Figure 7(c) shows endosomes in a BEAS-2B cell, with individual endosomes clearly visible throughout the cell.

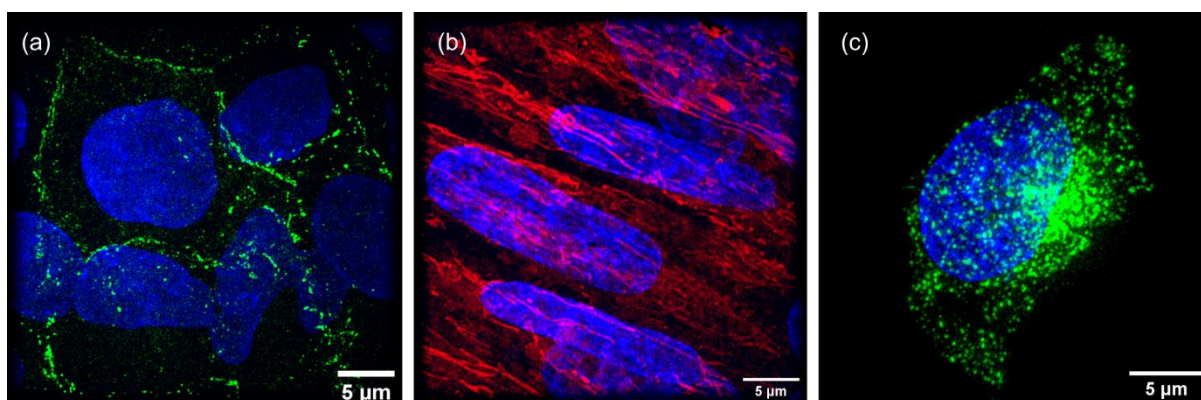


Figure 8. SIM images of fluorescent labelled lung fibroblasts and epithelial cells. (a) E-Cadherin (green) expression in A549 cells cultured at the air-liquid interface. (b) Mitochondria (red) in HFL1 cells exposed to uncoated soot particles at the air-liquid interface. (c) Endosomes (transferrin) in BEAS-2B cells exposed to alpha-pinene-coated soot particles at the air-liquid interface.

4.3.5 Cell-seeded tissue scaffolds

The high degree of light scattering within the lung tissue scaffolds made capture of high-quality image data deep inside the sample challenging. This is illustrated in Figure 9(a) which shows an XZ image slice through a typical 3D LSM data set, where it is only possible to resolve the scaffold structure and detect the presence of cells within the first few 10s of μm beneath the top surface. Figure 9(b) is a plot of the normalised variance for each image plane versus depth within the sample, and shows an exponential decrease with increasing penetration depth. To increase depth penetration we applied the CUBIC tissue clearing protocol [21] to the mounted scaffold sections prior to imaging. Figure 9(c) and (d) illustrate how this dramatically increases image quality inside the samples, primarily by matching the refractive index of the imaging buffer to the scaffold, with fibres clearly resolved throughout the entire ($\sim 350 \mu\text{m}$ thickness of the scaffold).

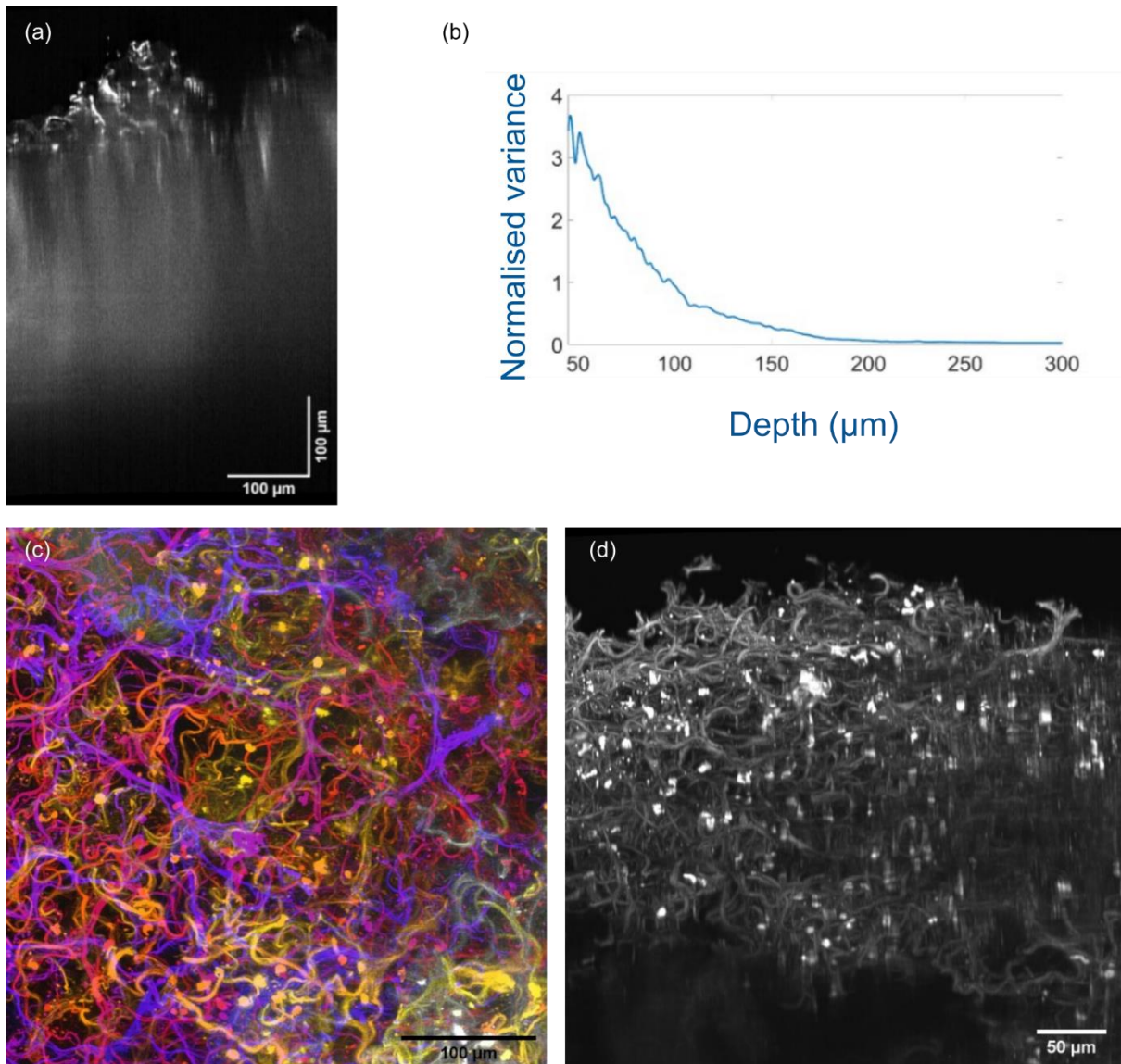


Figure 9. LSFM of fibroblasts cultured in a decellularised lung tissue scaffold. (a) XZ image slice from the full 3D image stack of an uncleared tissue illustrating loss of image quality with imaging depth due to light scattering. (b) Normalised variance (a measure of image sharpness) as a function of depth into the scaffold for the dataset shown in (a). (c) Colour depth (z) projection of LSFM 3D image stack for a piece of the same scaffold type cleared using CUBIC-1. (d) XZ maximum intensity project (along the Y dimension) for the dataset shown in (c). Individual cells (cytopainter red) are visible as bright puncta.

4.3.6 Visualisation of intracellular particle uptake and localisation

To visualise the intracellular uptake and localisation of particles we added a dilute suspension of 100 nm diameter silica particles labelled with the fluorescent dye Dy-557. Figure 10(a) shows a group of particles on the substrate of the sample chamber, illustrating how the higher spatial resolution of SIM allows closely-spaced particles, indivisible in the diffraction-limited (DL) image, to be resolved as discrete objects. Figure 10(b) shows orthogonal maximum intensity projections through a SIM z-stack of a BEAS-2B cell incubated with the same particles for four hours. Although many of the particles lie within the (lateral and axial) projected area of the cell, it is difficult to determine whether they have been internalised or are attached to the outside of the plasma membrane. Approaches for determining whether individual particles have been internalised within a cell



include: adding a chemical agent to quenching the fluorescence from extracellular particles; staining the plasma membrane; and the use of pH-sensitive fluorescent particles which change colour within acidic intracellular vesicles.

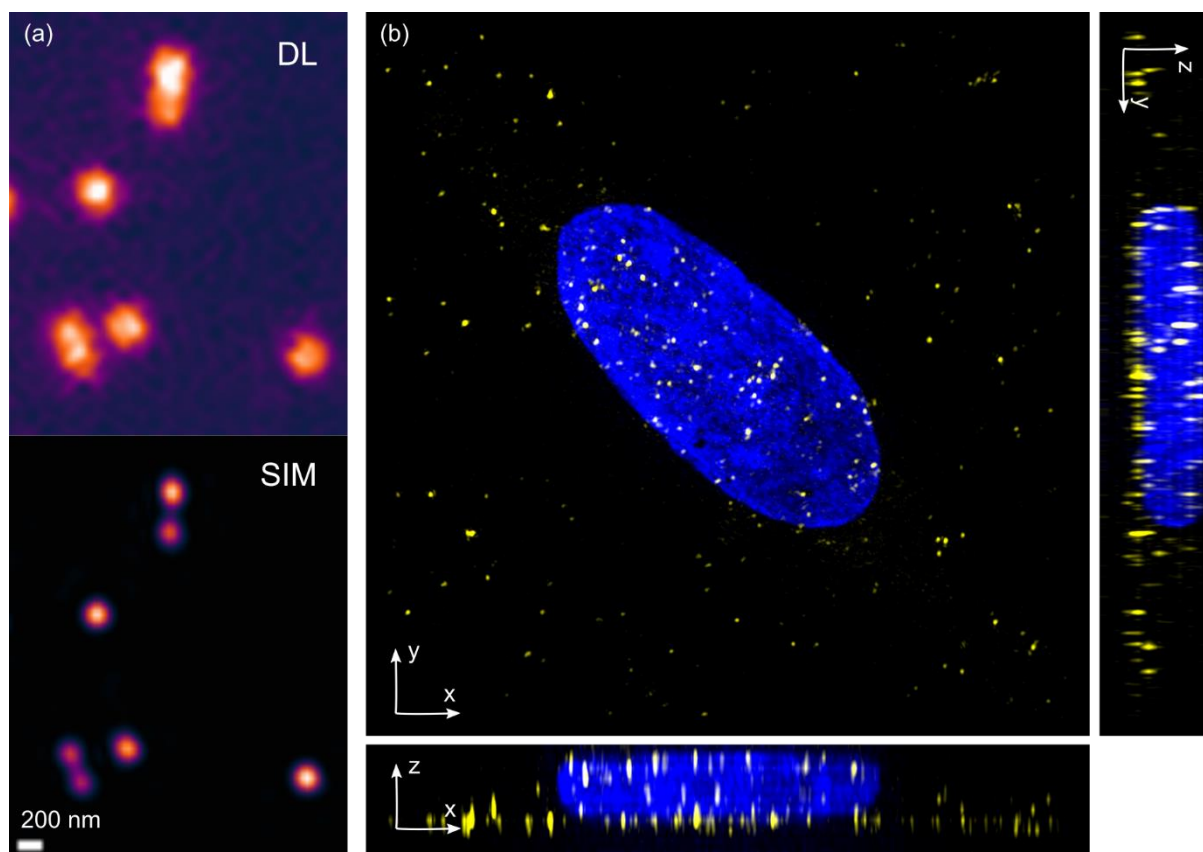


Figure 10. Visualisation of fluorescent silica particles using SIM. (a) Diffraction-limited (DL) epifluorescence (top panel) and SIM (lower panel) images of 100 nm diameter silica microspheres labelled with Dy-557.

Note, closely spaced particles which cannot be resolved in the DL image, are clearly resolved in the SIM image. (b) Orthogonal maximum intensity projections through SIM image data showing a BEAS-2B cell fixed after 4 hours of incubation with the same silica microspheres.

4.3.7 Summary

This section has described the application of optical, principally fluorescence, microscopy techniques for visualising respiratory cell systems, how they are perturbed by exposure to particulate matter and the particles themselves. Our results highlight the importance of matching the sample preparation protocol and the imaging technique to both the sample type and the method of particle exposure. Super-resolution SIM is particularly well-suited to high-resolution imaging of cellular organelles such as mitochondria, membrane proteins and mitochondria as well as fluorescently labelled particles. However, SIM suffers from a relatively limited depth penetration and small field of view, limiting its application to imaging small number of cells cultured on coverglass (or similar) substrates and Transwell membranes. CLSM offers a larger field of view, allowing imaging of larger cell populations at the expense of spatial resolution. It is likely, although as yet untested, that by employing an objective lens with an immersion medium which is closely matched to the sample (such as water, glycerol or silicone oil) and chemical clearing the sample, CLSM may also be suitable for deep imaging inside re-cellularised lung tissue scaffolds. However, with its superior imaging speed and lower specimen light exposure LFSM is expected to offer significant performance advantages for longer duration time lapse imaging studies.



Due to delays because of the Covid 19 pandemic, the project could only partly achieve the objective of advancing particle imaging techniques (Objective 4).

5 Impact

The Kick Off meeting took place at the Federal Institute of Technology in Zurich (ETH Zürich), Switzerland, between 20 and 21 June 2019. Furthermore, a stakeholder committee was formed early in the project. The members' interests span the range of topics within the project. They are: Swiss Federal Laboratories for Materials Science and Technology (EMPA), University of Basel, University of Bern, University of Applied Sciences Northwestern Switzerland, Bundesanstalt für Materialforschung und -prüfung (BAM), Jing Ltd. (instrument manufacturer), NRC Canada and two representatives from the Swiss Federal Office for the Environment (Section "Traffic" and Section "Air Quality").

The project website has been created, at <http://empir.npl.co.uk/aerotox/>, and is regularly updated.

During the lifetime of the project, the consortium partners presented 18 oral or poster presentations at different European and national conferences. Eleven peer-reviewed papers and one Master's thesis have already been published, 1 more manuscript has been submitted and 2 are currently being drafted.

Several other dissemination activities including seminars, workshops, a Bachelor Thesis at Lund University and a Master's Thesis at METAS/EPFL have taken place. In particular, the NACIVT aerosol deposition chamber was exhibited at the ETH Conference on combustion-generated nanoparticles held in June 2019 at ETH Zurich, Switzerland. Consortium members have contributed directly to the EURAMET TC-MC meeting held at METAS in February 2020 and are also in close contact with regulatory agencies, such as the Swiss Federal Office for the Environment.

A successful stakeholder workshop was hosted by Lund University November 2022. The *In vitro respiratory toxicology: lung models, exposure methods and analytical techniques* workshop brought together leading researchers who are applying in vitro toxicological techniques to investigate the effects of exposure to air pollution on human health. The workshop was held at the Pufendorf Institute, Lund University, Sweden and was also available online.

Impact on industrial and other user communities

The novel oxidation flow reactor (OFR), which has been developed by FHNW and validated by METAS, is currently commercialised by FHNW and has already sold four units for use outside the framework of this project. Combined with a soot generator, such as a mini CAST or mini inverted burner, the OFR can produce a wide range of well-defined "fresh" and "aged" combustion aerosols, which can be applied in the field of toxicology, atmospheric sciences, calibration of common air-quality monitoring instrumentation (e.g. absorption photometers) and filter testing.

As an example, an international inter-comparison of commercial and prototype aerosol absorption instruments and BC absorption photometers took place at METAS in September 2020 with participation from national metrology institutes, academia and industrial partners. All instruments were exposed simultaneously to a series of "fresh" and "aged" (i.e. coated with secondary organic matter) soot aerosols. The goal of the inter-comparison was to characterise the performance of various BC monitors in a controlled and reproducible way, help identify measuring artefacts, and provide feedback to our industrial partners on how to improve the design of the prototype absorption instruments.

Impact on the metrology and scientific communities

Our studies indicate that the use of ALI exposure on epithelial cells with the NACIVT chamber enables i) a more realistic particle dose and ii) a more accurate determination of the particle dose compared to submerged cell studies. Moreover, inter-comparison studies between cells cultured in 2D compared to 3D scaffolds and PCLS (which mimic the complex in vivo condition) indicate that the ECM microenvironment has an important role in modulating cellular responses involving cytokine and growth factor release. Changes in cell viability appear to be similar in vitro and ex vivo over time.



The new portable aerosol homogeniser developed in the project can be a useful tool in several areas, e.g. for laboratory studies using synthetic aerosols, instrument calibration and aerosol measurement at industrial and occupational settings. METAS has already sold one homogeniser along with custom-made isokinetic sampling units to a European institute for research and development purposes.

Impact on relevant standards

The project Consortium participated in international (ISO TC24/ SC4/ WG 9 & 12 and ISO TC172/ SC5/ WG 10) and national standardisation (BSI CPW/172) bodies where they provided input for the revision of relevant standards. The development of a portable aerosol mixing chamber has been within ISO TC24/ SC4/ WG 9 in view of the upcoming revision of the ISO standard 21501-1 on aerosol spectrometers (also known as optical particle sizers). Moreover, should new metrics, such as Black Carbon, particle number concentration etc., be found to correlate with adverse cellular responses consistent with the causal pathways associated with acute and chronic health effects, the calibration method developed by Kalbermatter et al. (see publication list below) could contribute to the development of entirely new standards.

Project partner NPL were also active in the light microscopy section committee of the Royal Microscopical Society (RMS) and a member of the QUAREP-LiMi (Quality Assessment and Reproducibility for Instruments & Images in Light Microscopy) consortium. For the former, NPL have contributed definitions to a new dictionary of light microscopy terms and for the latter they are particularly involved in working group 5, which is working to develop recommendations for the measurement of lateral and axial resolution in fluorescence microscopy. In ISO TC172/ SC5/ WG 3 NPL are working on a revision of ISO 10943:2020 – vocabulary for light microscopy.

Longer-term economic, social and environmental impacts

This project will support improvements to air quality data by reducing the measurement uncertainties for key air pollutants. This will be achieved through the newly developed instruments which can serve as transfer standards for the calibration of common air-quality monitoring systems and by extending the calibration and quality assurance procedures for emerging analytical techniques that are not yet adequately standardised.

Improving our understanding of the role of air pollutants in disease is essential in order to develop effective public health measures and reduce the exposure of the population to the most harmful components of ambient PM. The outputs from this project may also support a more targeted action on health-relevant components/properties, and promote the revision of air quality legislation, as well as extending the current legal framework to include metrics beyond PM mass concentration. Considering the enormous costs arising from hospitalisation and premature deaths, particularly in densely populated cities that constitute pollution hotspots, the protection of public health should also lead to substantial financial benefits.

6 List of publications

- Anna Löfdahl, Andreas Jern, Samuel Flyman, Monica Kåredal, Hanna L Karlsson and Anna-Karin Larsson-Callerfelt, "Silver Nanoparticles Alter Cell Viability Ex Vivo and in Vitro and Induce Proinflammatory Effects in Human Lung Fibroblasts", *Nanomaterials* 2020, 10(9), 1868, <https://doi.org/10.3390/nano10091868>
- Andrea Giordano, CFD simulation of an aerosol mixing chamber, EPFL Master's Thesis, 2020, <https://infoscience.epfl.ch/record/280815?ln=en>
- Mariam Bagher , Oskar Rosmark, Linda Elowsson Rendin, Annika Nybom, Sebastian Wasserstrom, Catharina Müller, Xiao-Hong Zhou, Göran Dellgren, Oskar Hallgren, Leif Bjerner, Anna-Karin Larsson-Callerfelt, and Gunilla Westergren-Thorsson, "Crosstalk between Mast Cells and Lung Fibroblasts Is Modified by Alveolar Extracellular Matrix and Influences Epithelial Migration", *Int. J. Mol. Sci.* 2021, 22(2), 506; <https://doi.org/10.3390/ijms22020506>
- Russell, C. & Shaw, M "mmSIM: An open toolbox for accessible structured illumination microscopy", *Philos. Trans. R. Soc. A*, <https://doi.org/10.1101/2021.01.18.427184>
- Karin Lovén, Julia Dobric, Deniz Bölükbas, Monica Kåredal, Darcy E. Wagner, Jenny Rissler, Christina Isaxon "Toxicological effects of zinc oxide nanoparticle exposure and the bias of the exposure system:



- an in vitro comparison between air-liquid interface and submerged exposure systems", *Nanotoxicology* 2021, 15(4), 494-510; <https://doi.org/10.1080/17435390.2021.1884301>
- Michaela N. Ess, Michele Bertò, Alejandro Keller, Martin Gysel-Beer, Konstantina Vasilatou, "Coated soot particles with tunable, well-controlled properties generated in the laboratory with a miniCAST BC and a micro smog chamber", *Journal of Aerosol Science* 2021, 157, 105820; <https://doi.org/10.1016/j.jaerosci.2021.105820>
 - Daniel Geißler, Nithiya Nirmalananthan-Budau, Lena Scholtz, Isabella Tavernaro, Ute Resch, "Analyzing the Surface of Functional Nanomaterials – How to Quantify the Total and Derivatizable Number of Functional Groups and Ligands", *Microchimica Acta* 2021, 188, Article number:321; <https://link.springer.com/article/10.1007/s00604-021-04960-5>
 - Kalbermatter et al., "Comparing black-carbon- and aerosol-absorption-measuring instruments – a new system using lab-generated soot coated with controlled amounts of secondary organic matter", *Atmos. Meas. Tech.*, 15, 561–572, 2022, <https://doi.org/10.5194/amt-15-561-2022>
 - Leni et al., "Role of Secondary Organic Matter on Soot Particle Toxicity in Reconstituted Human Bronchial Epithelia Exposed at the Air–Liquid Interface", *Environ. Sci. Technol.* 2022, 56, 23, 17007–17017, <https://doi.org/10.1021/acs.est.2c03692>
 - Horender et al. "A portable flow tube homogenizer for aerosol mixing in the sub-micrometre and lower micrometre particle size range", *Meas. Sci. Technol.* 33 114006 (2022), <https://iopscience.iop.org/article/10.1088/1361-6501/ac81a1/pdf>
 - Alejandro Keller, Daniel M. Kalbermatter, Kate Wolfer, Patrik Specht, Peter Steigmeier, Julian Resch, Markus Kalberer, Tobias Hammer & Konstantina Vasilatou (2022) The organic coating unit, an all-in-one system for reproducible generation of secondary organic matter aerosol, *Aerosol Science and Technology*, 56:10, 947-958, <https://doi.org/10.1080/02786826.2022.2110448>
 - Rosmark O, Ibáñez-Fonseca A, Thorsson J, Dellgren G, Hallgren O, Larsson Callerfelt A-K, Elowsson L and Westergren-Thorsson G (2022), A tunable physiometric stretch system evaluated with precision cut lung slices and recellularized human lung scaffolds. *Front. Bioeng. Biotechnol.* 10:995460. <https://doi.org/10.3389/fbioe.2022.995460>
 - Al-Rekabi Z., Larsson-Callerfelt A-K., Mudway I., Kåredal M., Rissler J., Elowsson L., Siddiqui N.S., Faruqi N., Dondi C., Shaw M. 2023. Uncovering the cytotoxic effects of air pollution with multi-modal imaging of in vitro respiratory models. *R. Soc. Open Sci.* 10: 221426. <https://doi.org/10.1098/rsos.221426>

This list is also available here: <https://www.euramet.org/repository/research-publications-repository-link/>